

THREE DIMENSIONAL COMPUTATION OF TAYLOR-COUETTE FLOW

Naoki Matsumoto (松本 直樹)

The Institute of Computational Fluid Dynamics, Tokyo, Japan

Susumu Shirayama (白山 晋)

The Institute of Computational Fluid Dynamics, Tokyo, Japan

Kunio Kuwahara (桑原 邦郎)

The Institute of Space and Astronautical Science, Tokyo, Japan

1. Abstract

Three dimensional incompressible Navier-Stokes equations are solved numerically for Taylor-Couette flow with the outer cylinder at rest. The wavelength of supercritical Taylor vortices created through an impulsive start of the inner cylinder is studied. The evolution of Taylor-vortex structure is visualized and can be investigated precisely. The results are compared with experimental results. Both results agree well qualitatively.

2. Introduction

Experiments for flows between concentric cylinders were performed by Burkhalter & Koschmieder (1974). They measured the wavelengths of steady-state vortices that resulted from impulsively starting the inner cylinder from a state of rest with the outer cylinder held fixed. According to these experiments, the wavelength initially decreased up to $R/R_c \approx 4$ (R_c : Critical Reynolds number from linear theory). Beyond $R/R_c \approx 4$, the wavelength increased with increasing R . The objective of the present work is to examine this problem. The visualization and the measurements of the 3-dimensional flow are very difficult, and there seems to be no current theory available for such strongly nonlinear flows. Therefore it appears that numerical simulation is the only useful tool for our purpose. Neitzel (1984) performed the axisymmetric computation of the incompressible Navier-Stokes equations in finite-length concentric cylinder geometry. But the wavelength did not increase for $R/R_c > 4$. So we have performed 3-dimensional computation and compared the results with the experiments.

3. Numerical Method

Consider a pair of concentric cylinders of radii a and b and height h . We assume the gap between the cylinders to be filled with a viscous incompressible fluid of kinematic viscosity ν . The entire system is assumed to be in an initial state of rest. At time $t = 0$, the inner cylinder at radius $r = a$ is impulsively set into rotation with angular velocity Ω while the outer cylinder at $r = b$ is held fixed. The rigid endwalls at $z = 0, h$ are assumed to be attached to the inner cylinder and therefore begin to rotate with it at $t = 0$. The variables are made dimensionless using the scales $d \equiv b - a$, Ωd and Ω^{-1} for length, speed and time respectively.

Numerical method is based on the MAC method except treating pressure. The incompressible Navier-Stokes equations are expressed as follows:

$$\frac{\partial \mathbf{v}}{\partial t} + (\mathbf{v} \cdot \nabla) \mathbf{v} = -\text{grad} p + \frac{1}{R_e} \Delta \mathbf{v} \quad (1)$$

$$\text{div} \mathbf{v} = 0 \quad (2)$$

These equations are written in a generalized coordinates system and solved by finite-difference method. Applying the operator $\text{grad} \cdot \text{div}$ to the both

sides of equation (1), we obtain the Poisson equations for gradient of pressure:

$$\Delta \mathbf{P} = -\text{grad} \cdot \text{div}(\mathbf{v} \cdot \nabla) \mathbf{v} + \text{grad} R + \text{rot} \cdot \text{rot} \mathbf{P} \quad (3a)$$

where

$$\mathbf{R} = -\frac{\partial \mathbf{D}}{\partial t} + \frac{1}{R_e} \mathbf{D}, \quad \mathbf{P} = \text{grad} p, \quad \mathbf{D} = \text{div} \mathbf{v} \quad (3b)$$

and the formula of vector analysis $\text{grad} \cdot \text{div} \mathbf{X} = \Delta \mathbf{X} + \text{rot} \cdot \text{rot} \mathbf{X}$ is used. The time derivative, $\partial \mathbf{D} / \partial t$, is evaluated by forcing $\mathbf{D}^{n+1} = 0$, i.e.,

$$\frac{\partial \mathbf{D}}{\partial t} \simeq -\frac{\mathbf{D}^n}{\Delta t}$$

The boundary conditions for (1), (3) are as follows (dimensional variables):

$$u = V, \quad v = 0, \quad w = 0$$

$$P_r = \frac{1}{R_e} \frac{\partial^2 u}{\partial r^2} + \frac{V^2}{a}, \quad P_\theta = \frac{1}{R_e} \frac{1}{a^2} \frac{\partial^2 v}{\partial \theta^2}, \quad P_z = \frac{1}{R_e} \frac{\partial^2 w}{\partial z^2}$$

at $r=a$

$$u = 0, \quad v = 0, \quad w = 0$$

$$P_r = \frac{1}{R_e} \frac{\partial^2 u}{\partial r^2}, \quad P_\theta = \frac{1}{R_e} \frac{1}{b^2} \frac{\partial^2 v}{\partial \theta^2}, \quad P_z = \frac{1}{R_e} \frac{\partial^2 w}{\partial z^2}$$

at $r=b$

$$u = r\Omega, \quad v = 0, \quad w = 0$$

$$P_r = \frac{1}{R_e} \frac{\partial^2 u}{\partial r^2} + \frac{u^2}{r}, \quad P_\theta = \frac{1}{R_e} \frac{1}{r^2} \frac{\partial^2 v}{\partial \theta^2}, \quad P_z = \frac{1}{R_e} \frac{\partial^2 w}{\partial z^2}$$

at $z=0, h$

(u, v, w) are the velocity components in the directions given by the cylindrical coordinates (r, θ, z) , and (P_r, P_θ, P_z) are the components of \mathbf{P} in each direction. The Poisson equations for gradient of pressure are solved by successive over relaxation. Dealing with gradient of pressure instead of pressure, the Neumann problem is transformed to the Dirichlet problem

and the convergence becomes good. The Euler semi-implicit scheme is used for the time integration of velocity. (All but the convective velocity are computed implicitly.) All spatial derivatives except the nonlinear terms are approximated by central differences. The nonlinear terms are approximated by the third-order upwind scheme:

$$\left(u \frac{\partial u}{\partial x}\right)_i = u_i \frac{-u_{i+2} + 8(u_{i+1} - u_{i-1}) + u_{i-2}}{12h} + |u_i| \frac{u_{i+2} - 4u_{i+1} + 6u_i - 4u_{i-1} + u_{i-2}}{4h}$$

We assume the flow to be symmetric about the midplane to reduce the size of the computational domain. This restricts the flow to have an even number of vortices, which is the case normally observed in the laboratory. A grid system is shown in fig.1. Constant grid spacing is used in each direction. The computations were done on Japanese supercomputer NEC SX2.

4. Results

There are three nondimensional parameters:

$$\eta = b/a \quad (\text{Radius ratio})$$

$$\gamma = h/d \quad (\text{Ratio of height and gap})$$

$$R_e = \Omega d^2 / \nu \quad (\text{Reynolds number})$$

$$(R_c = 31.03)$$

$$\text{cf) } Ta = \frac{2\eta^2}{1 - \eta^2} R_e^2 \quad (\text{Taylor number})$$

η is fixed at 0.727, and γ is fixed at 23.35 to correspond with the experiment of Burkhalter & Koschmieder. The computations are performed for four cases $R/R_c = 2, 3, 4, 6$ (R_c : Critical Reynolds number from linear theory).

Steady-state

Figure.2 shows instantaneous streamlines in the vertical surface for $R/R_c = 2, 3, 4, 6$. Wavelengths of steady state results are plotted in fig.3 with the

comparison of the experimental and other numerical results. The wavelength λ is defined as follows:

$$\lambda = \frac{\gamma - 2\epsilon}{N}$$

where ϵ is the length of the endcell, and N is the number of vortex-rings (=1/2 number of cells) excluding endcells. The agreement is not good quantitatively. Probably the main reason is that the experiment is not a perfect impulsive start. According to other experiments of them, the wavelength depends on the history of the acceleration. (Table 1) And another reason is from the numerical error due to the discontinuity in the boundary conditions at the axial end plates. However wavelengths of computational results are within the theoretical limit (Fig.4). The quantitative agreement is not good, but the agreement is good qualitatively. Both wavelengths of the computational results and the experiments increase for $R/R_c > 4$.

Evolution of Taylor-vortices

Why does the wavelength increase for $R/R_c > 4$? We have investigated the time-evolution of vortices.

(1) $R/R_c = 3$

At first, a vortex develops from the end-boundary by Ekman pumping, induces next vortex, and propagates up. Finally vortices fill the gap between the cylinders and go to the steady-state. Flow is axisymmetric during this procedure. Fig.5a shows the instantaneous streamlines in the vertical surface. Fig.5b shows the contour of the vorticity normal to the surface. It is found that the vorticity is supplied from the inner boundary.

(2) $R/R_c = 6$

Vortices fill the gap between the cylinders by the same process with case(1). However, this is not the steady-state. This state makes a transition to the state in which there are large Taylor vortices. Fig.6a shows the instantaneous streamlines in the vertical surface. During the transition we found that wavelengths of vortices gradually increase by vortex-connection. This feature is not found in the axisymmetric computation of incompressible Navier-Stokes equations by Neitzel(1984).

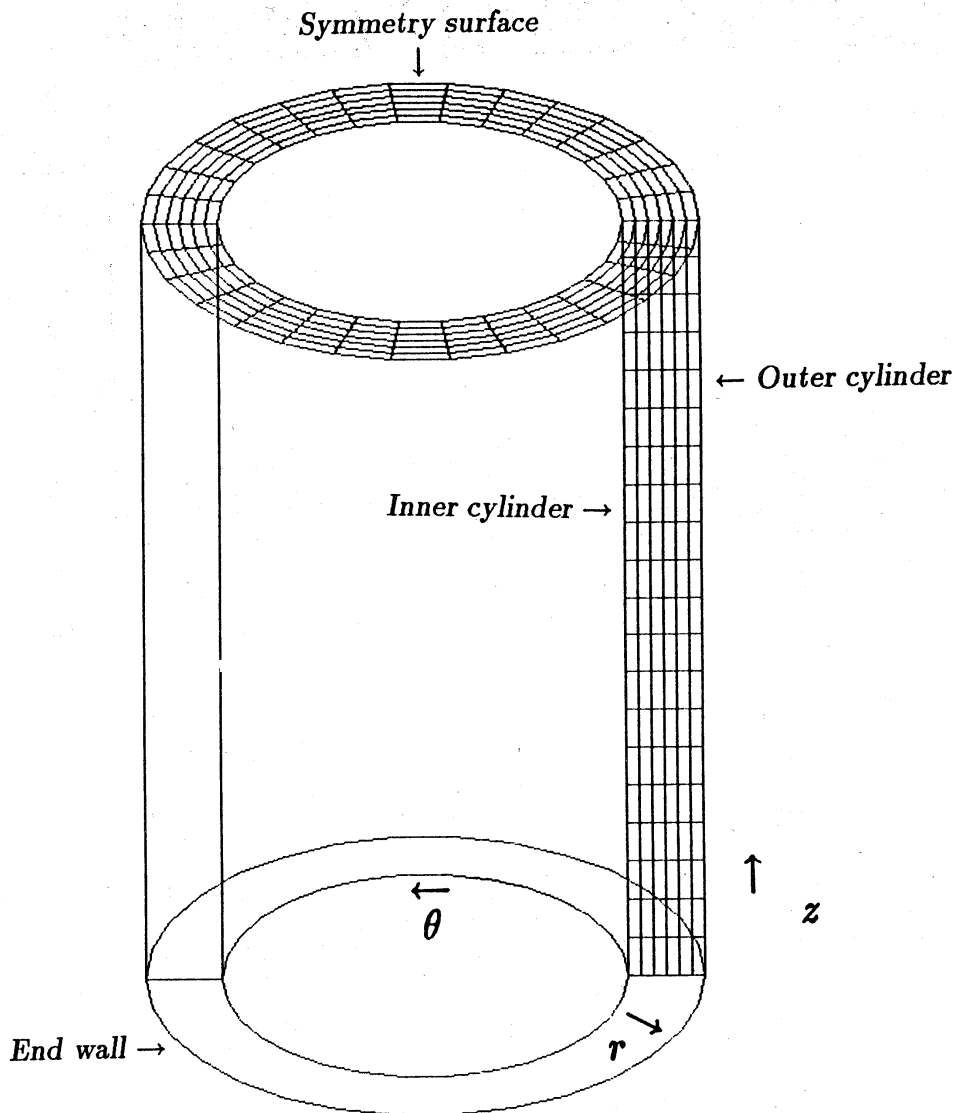
So the transition are probably due to the non-axisymmetric effects. Fig.6b shows the contour of the vorticity normal to the surface. It is found that the vortices which have the same sign are connecting.

5. Conclusion

The wavelength of Taylor vortices through an impulsive start increases for $R/R_c > 4$ by vortex-connection, and this feature was not found by axisymmetric computation by Neitzel (1984). So this is the non-axisymmetric effect.

REFERENCES

- [1] S.Chandrasekhar : *Hydrodynamic and Hydromagnetic Stability* (Oxford University Press,Oxford,1961) p.303
- [2] S.Kogelman & R.C.DiPrima : Stability of spatially periodic supercritical flows in hydrodynamics. *Phys.Fluids* 13 (1970)
- [3] J.E.Burkhalter & E.L.Koschmieder : Steady supercritical Taylor vortices after sudden starts. *Phys.Fluids* 17,1929 (1974)
- [4] G.P.Neitzel : Numerical computation of time-dependent Taylor vortex flows in finite-length geometries. *J.Fluid Mech.*141,51 (1984)
- [5] T.Kawamura & K.Kuwahara : Computation of high Reynolds number flow around a circular cylinder with surface roughness. AIAA papaer 84-0340 (1984)



GRID POINTS = $30 \times 31 \times 101$

Fig.1 Grid system

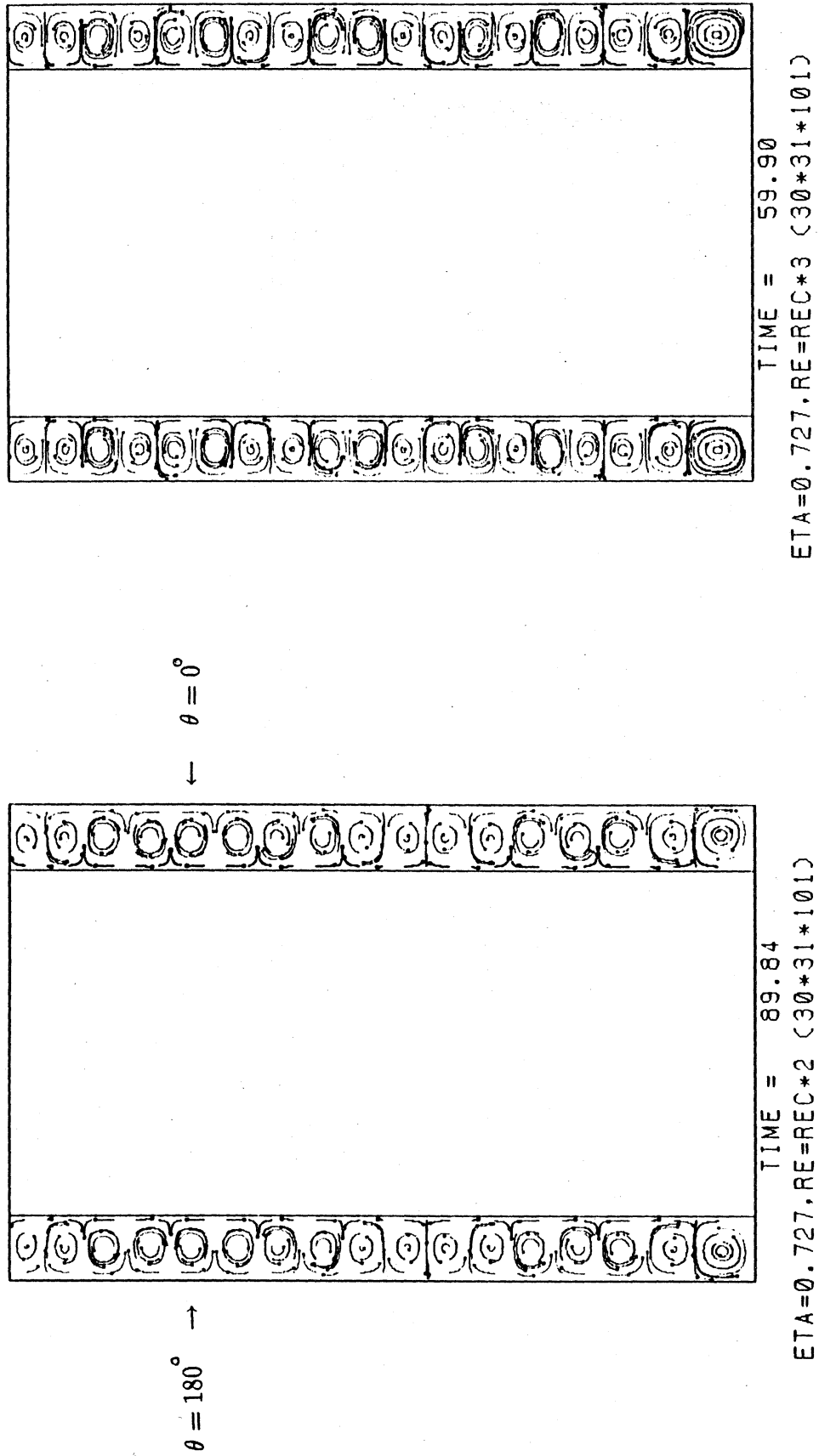
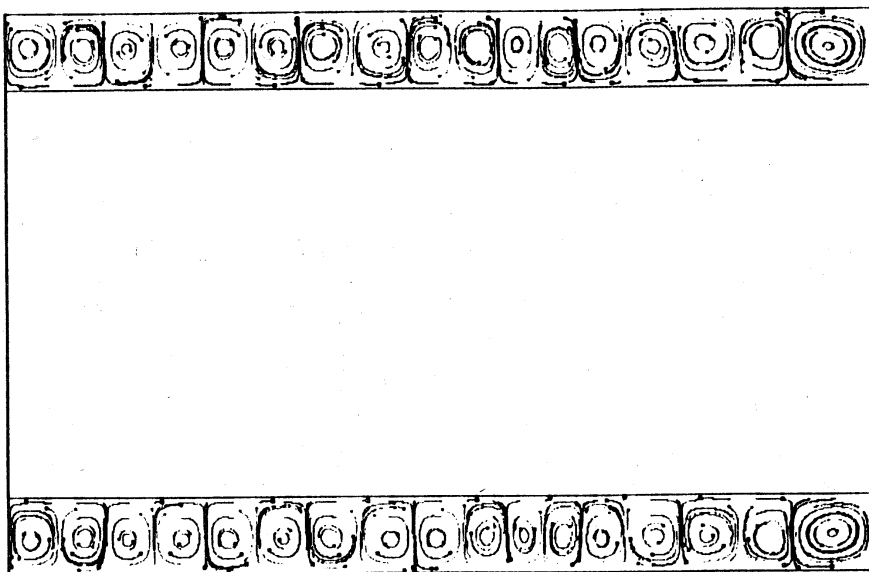
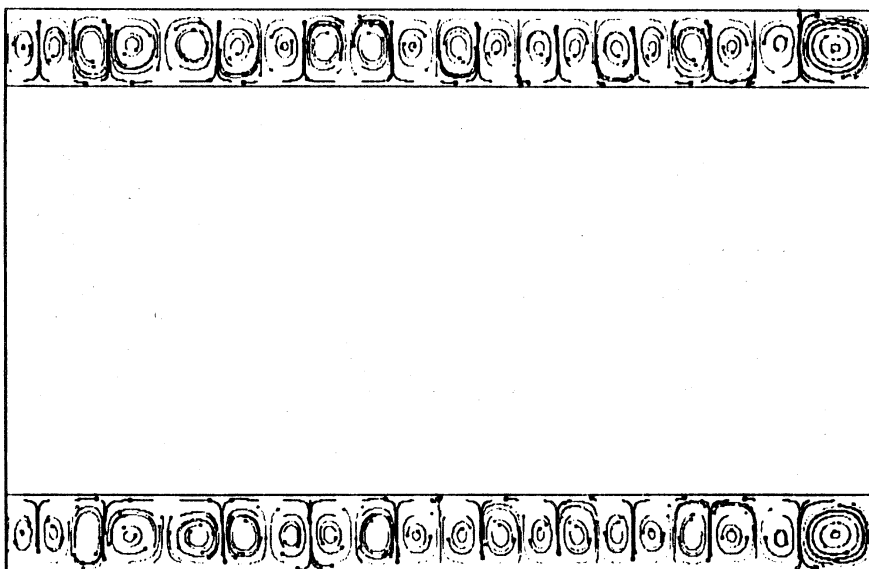


Fig.2 Instantaneous streamlines in the vertical surface for $R/R_c = 2, 3, 4, 6$



TIME = 109.80
ETA=0.727, RE=REC*6 (30*31*101)



TIME = 79.86
ETA=0.727, RE=REC*4 (30*31*101)

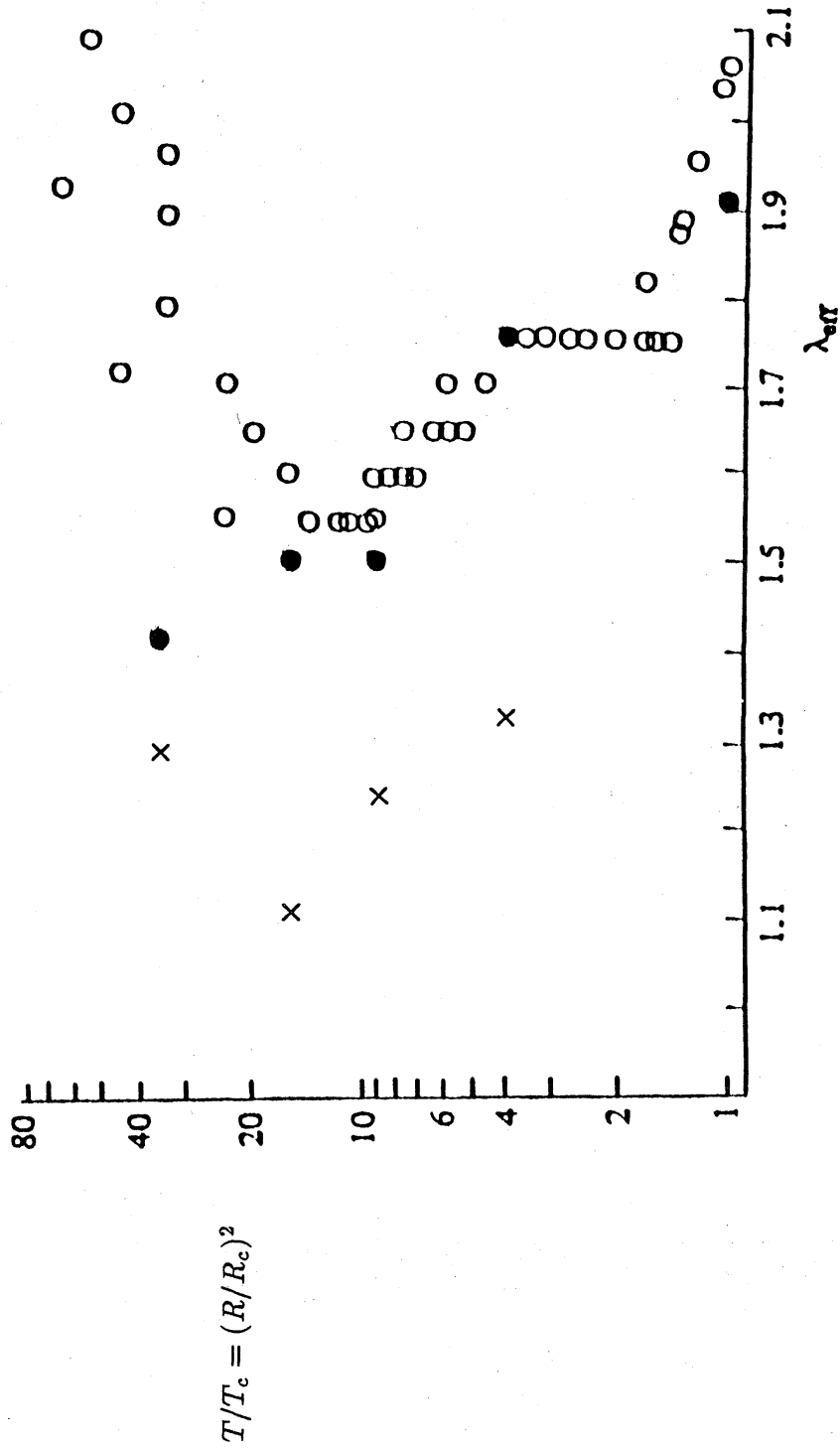


Fig.3 Wavelength versus Taylor number
 A) o: Experimental results by Burkhalter & Koschmieder¹⁾
 B) x: Present numerical results
 C) •: Numerical results of axisymmetric computation by Neitzel²⁾

Wavelength increases for $R/R_c > 4$ in A and B, but does not in C.

Δt (sec)	0.5	3.16	11.8	20.3	36.4	3600
\bar{N}	30.9 ± 0.7	29.3 ± 0.9	27.8 ± 0.6	27.8 ± 0.5	27.3 ± 0.6	25
$\bar{\lambda}_m$	1.65 ± 0.04	1.74 ± 0.05	1.84 ± 0.04	1.84 ± 0.03	1.87 ± 0.04	2.04

Table 1 Wavelengths after different acceleration periods at $T/T_c = 5.44$, resting end plates

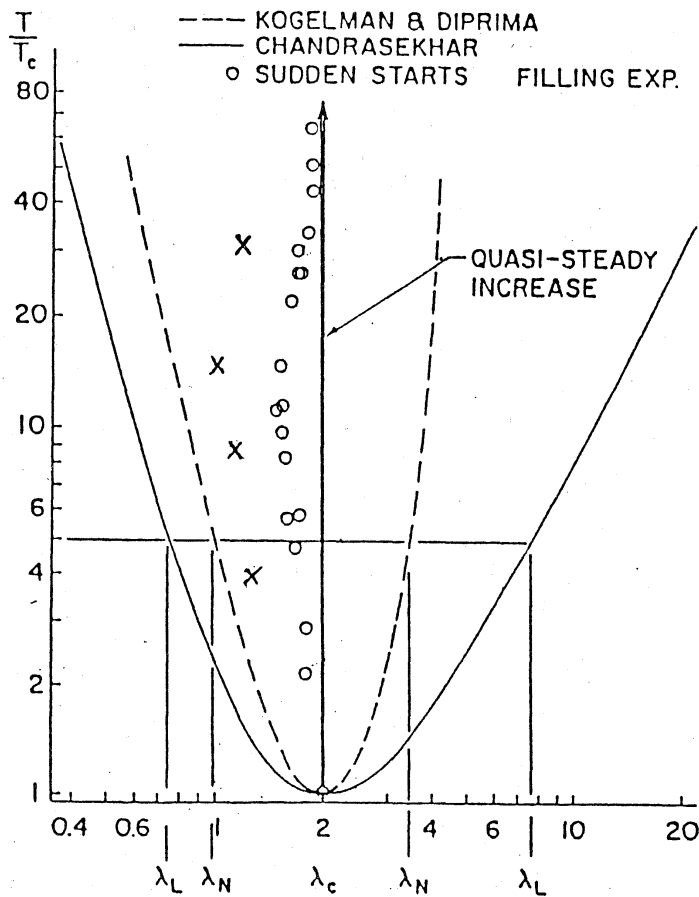
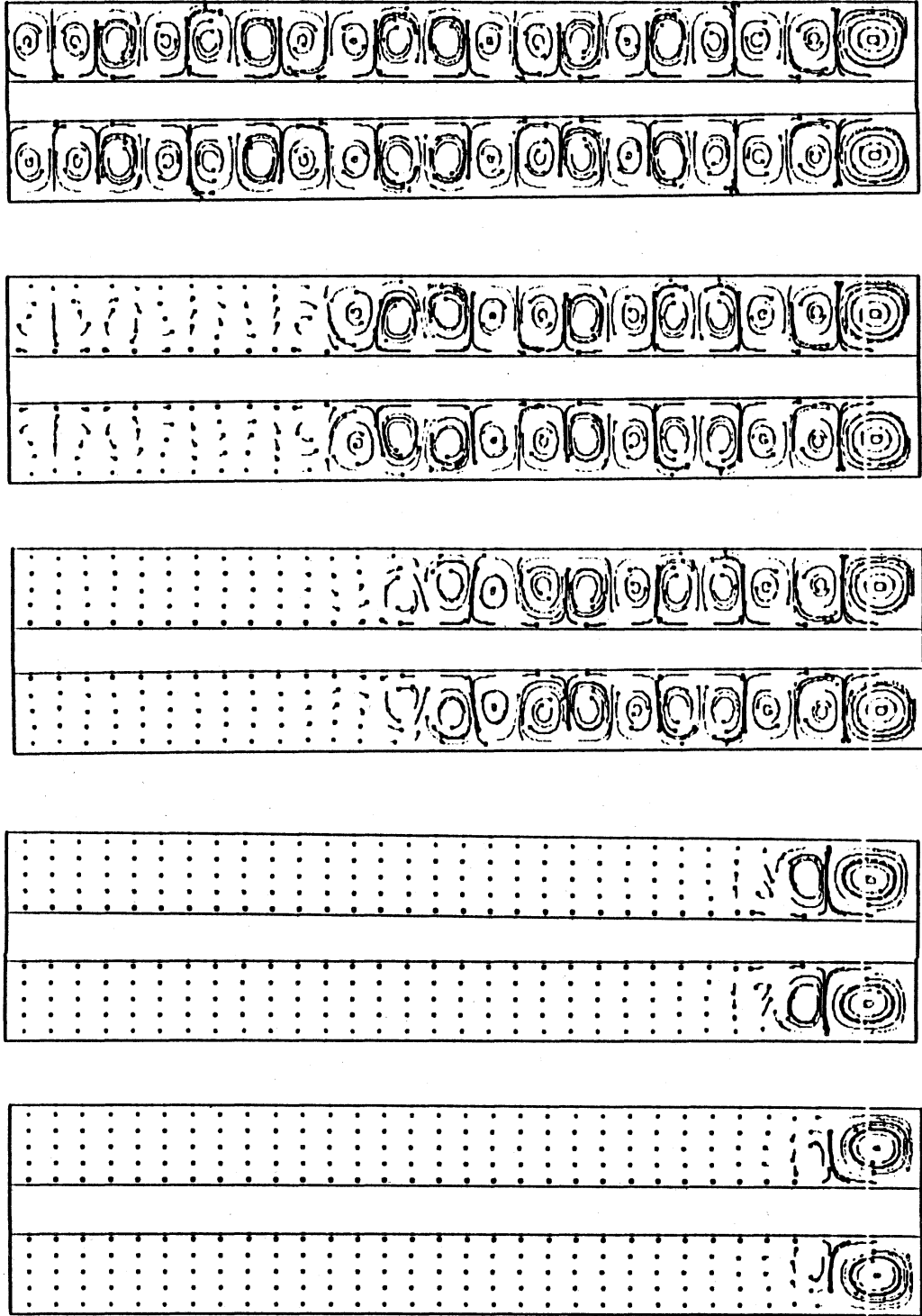


Fig.4 Stability diagram for supercritical Taylor vortex flow with the experimental results and numerical results

ETA=0.727, RE=REC*3 (30*31*101)



59.90

39.94

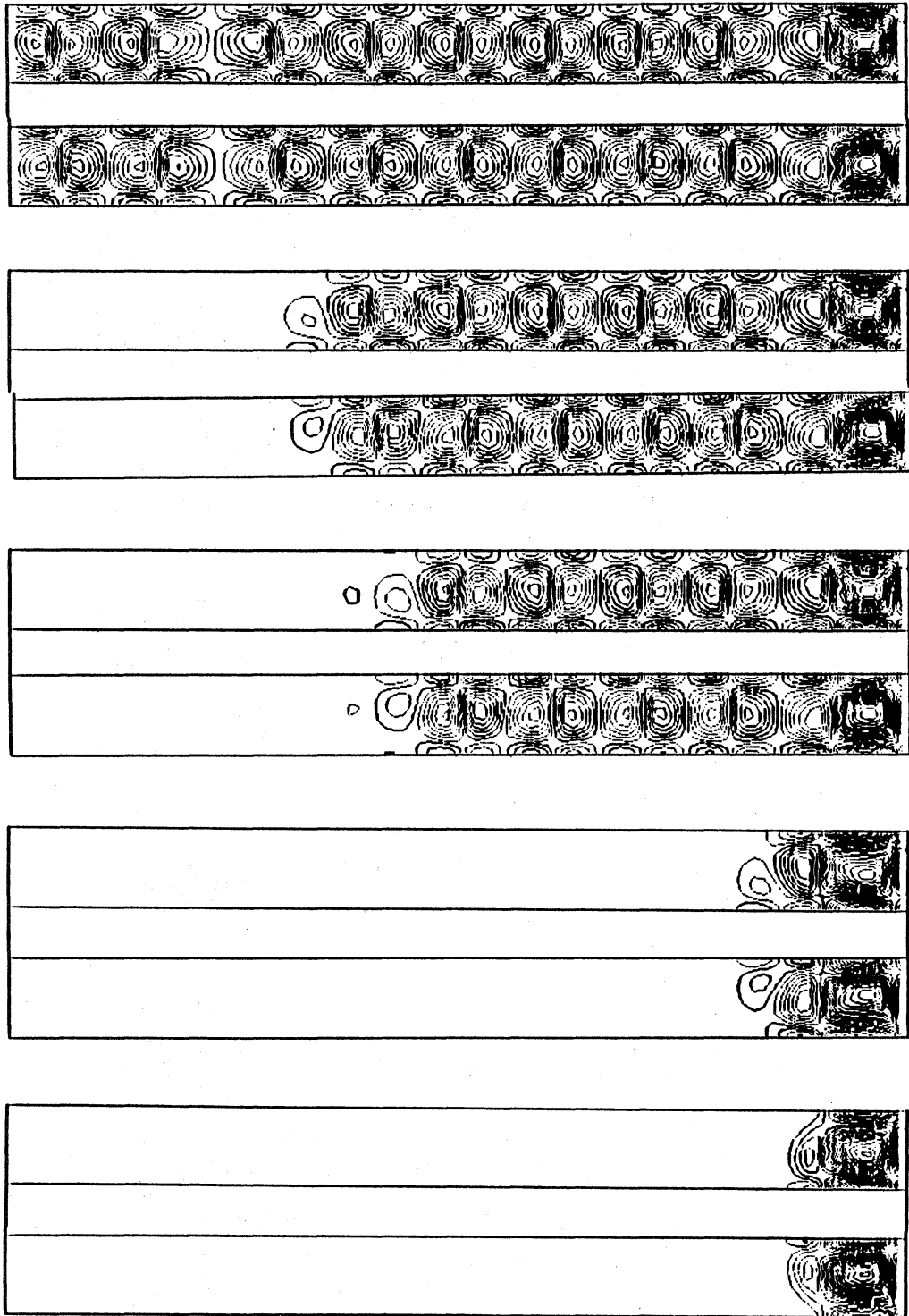
34.95

9.99

TIME = 4.99

Fig.5a Instantaneous streamlines in the vertical surface for $R/R_c = 3$

VORTICITY(NORMAL), RE=REC*3



59.90

39.94

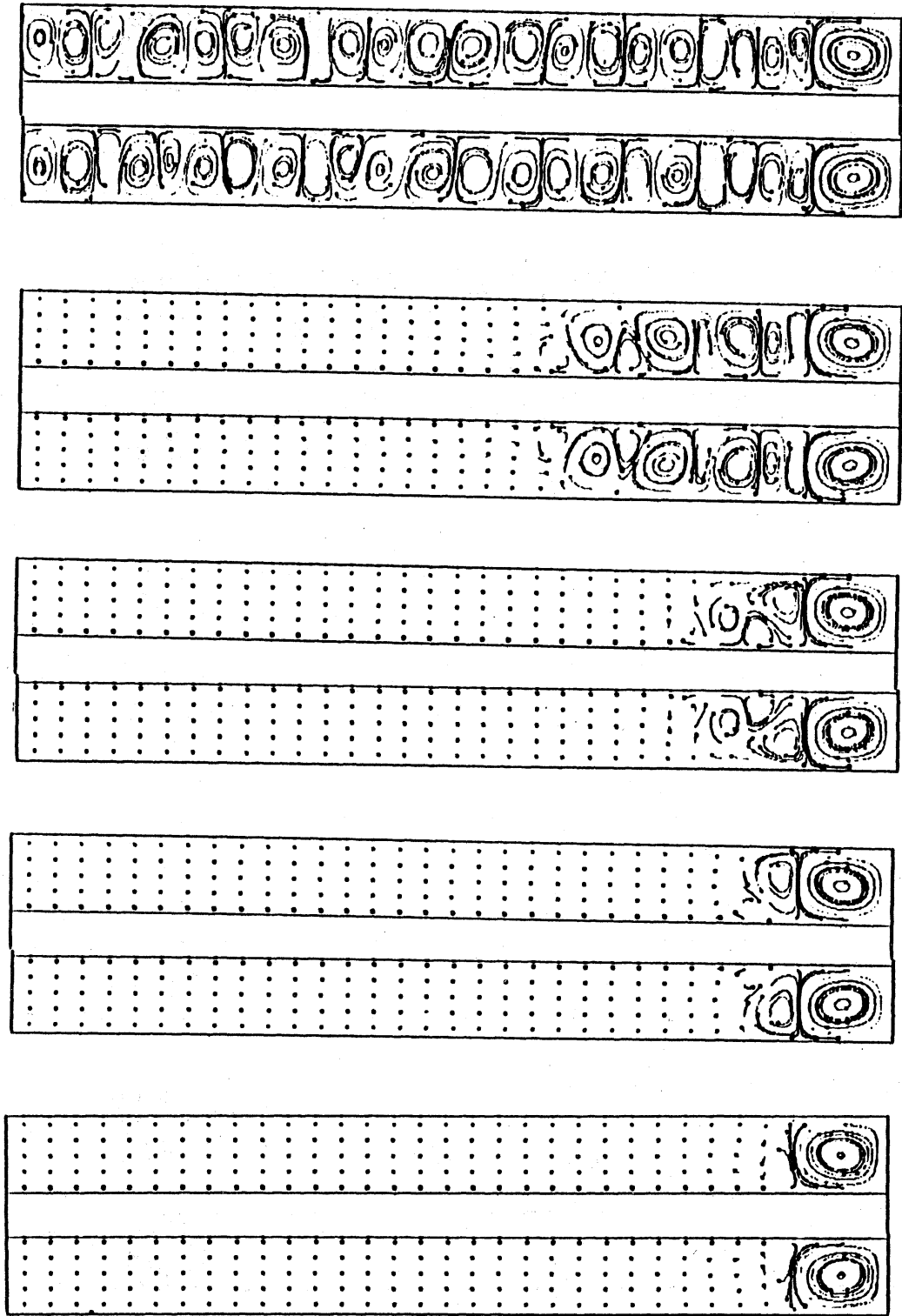
34.95

9.99

TIME = 4.99

Fig.5b Contour of vorticity normal to the surface for $R/R_c = 3$

ETA=0.727, RE=REC*6 (30*31*101)



39.94

24.97

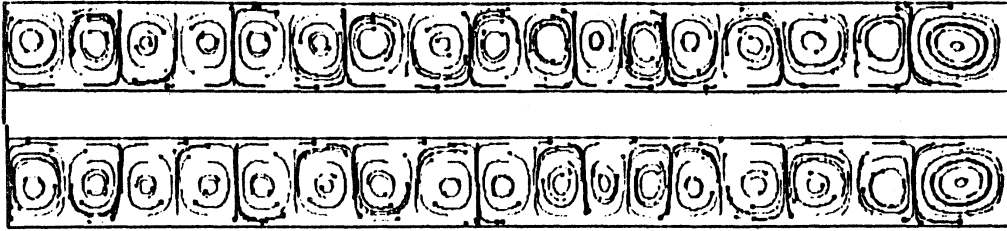
14.99

9.99

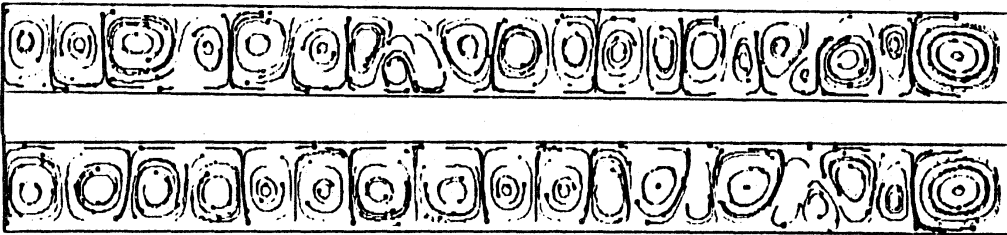
4.99

TIME =

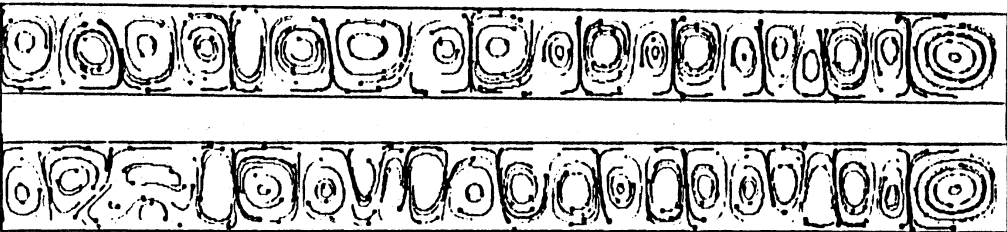
Fig.6a Instantaneous streamlines in the vertical surface for $R/R_c = 6$



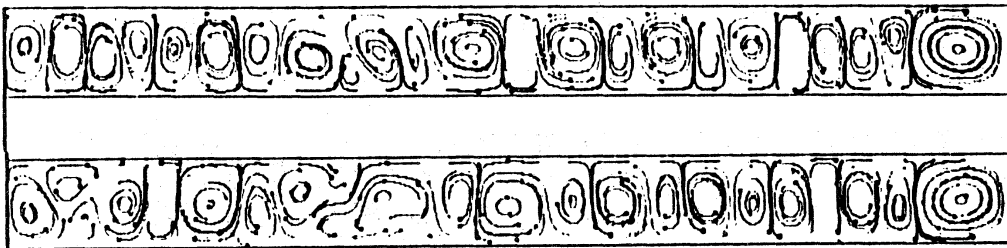
109.80



69.88



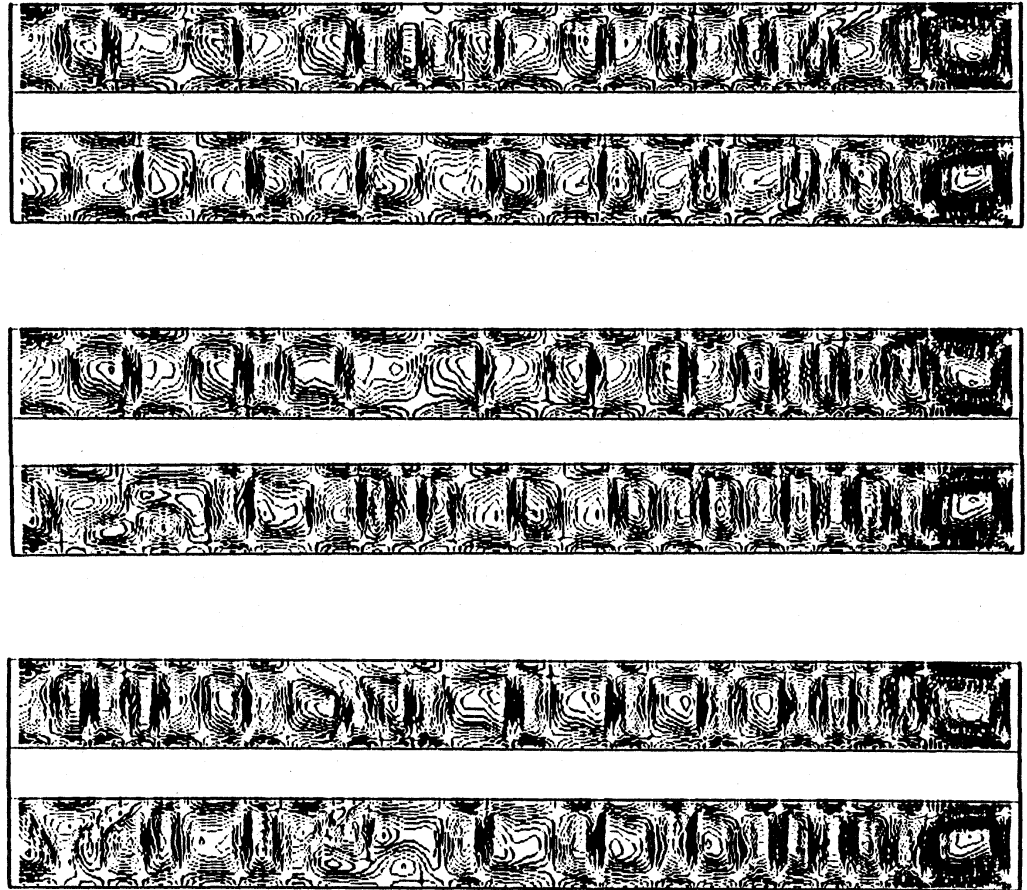
59.90



49.92

Transition occurs and flow becomes non-axisymmetric.

VORTICITY(NORMAL), RE=REC*6



TIME = 49.92 59.90 69.88

Fig.6b Contour of vorticity normal to the surface for $R/R_c = 6$